



Isothermal kinetics and thermal degradation of an aryl azo dye-containing polynorbornene

A.A. Joraid^{a,*}, S.N. Alamri^a, A.A. Abu-Sehly^a, S.Y. Al-Raqa^b, P.O. Shipman^c,
P.R. Shipley^c, A.S. Abd-El-Aziz^c

^a Department of Physics, Taibah University, Madinah, Saudi Arabia

^b Department of Chemistry, Taibah University, Madinah, Saudi Arabia

^c Department of Chemistry, The University of British Columbia Okanagan, Kelowna, British Columbia, Canada

ARTICLE INFO

Article history:

Received 24 August 2010

Received in revised form

11 December 2010

Accepted 15 December 2010

Available online 6 January 2011

Keywords:

Degradation

Polymer kinetics

Differential scanning calorimetry

Isothermal study

ABSTRACT

The kinetics involved in the thermal degradation of an aryl azo dye-containing polynorbornene was investigated by using isothermal DSC data. The activation energy of the degradation was found to be temperature dependent with two different values of 140 ± 5 and 21 ± 2 kJ mol⁻¹, and the Avrami exponent was observed to increase from 2 to 4 in the temperature range 573–608 K. The degradation mechanism follows the Avrami–Erofeev mechanism for solid state reaction models and it changes from A2 toward A4 for the same temperature range.

© 2011 Elsevier B.V. All rights reserved.

1. Introduction

There is an increasing demand for the development of azo dye based polymers, in light of their potential applications as photonic devices [1–9]. The azo group (–N=N–) is characterized by its reversible transformation from the more stable *trans* form to the less stable *cis* form by illumination with UV or visible light [9,10]. While, there are many studies on establishing the reaction mechanism of polymers, the kinetics of the decomposition has not been fully investigated.

As most polymers experience thermal degradation at high temperature, the study of the thermal degradation of polymers is important for understanding their usability, storage and recycling. Thermal analytic methods provide useful information in defining suitable processing conditions for these polymers and their applications, and obtain information on the relationships between thermal properties and polymer chain structure. The two main techniques used to investigate the thermal degradation of polymers are thermogravimetry (TG) and differential scanning calorimetry (DSC).

Thermal analysis by DSC is a rapid and convenient tool for studying the degradation kinetics of polymers. These studies can

be performed using isothermal or non-isothermal techniques. For isothermal measurements, the sample is quickly brought to a temperature above the glass transition temperature (T_g) and the heat evolved during the degradation process is recorded as a function of time. In contrast, for non-isothermal measurements the sample is heated at a fixed rate and the heat evolved is recorded as a function of temperature.

Knowledge of kinetic parameters, such as reaction order, activation energy, pre-exponential factor and rate constant, is one of the keys to determining reaction mechanisms in solid phases. The kinetic analysis of polymers has been considered by a numerous authors [11–25]. This study focuses on the degradation kinetics and the effect of temperature on the activation energy, pre-exponential factor and reaction order of an azo dye-containing polynorbornene by means of the isothermal methods.

2. Experimental methods

The polymer under investigation, Fig. 1, was prepared according to our previously reported methodology [11].

The DSC experiments presented in this paper were performed using a Shimadzu DSC-60 instrument with an accuracy of ± 0.1 K, under dry nitrogen supplied at a rate of 35 ml min⁻¹. In order to minimize temperature gradients, 3 mg samples were spread thinly across the bottom of standard aluminum sample pans followed by encapsulation. The temperature and enthalpy calibrations were

* Corresponding author at: Department of Physics, Taibah University, P.O. Box 3668, Madinah, Saudi Arabia. Tel.: +966 4822 6462; fax: +966 4823 3727.

E-mail address: aaljoraid@taibahu.edu.sa (A.A. Joraid).

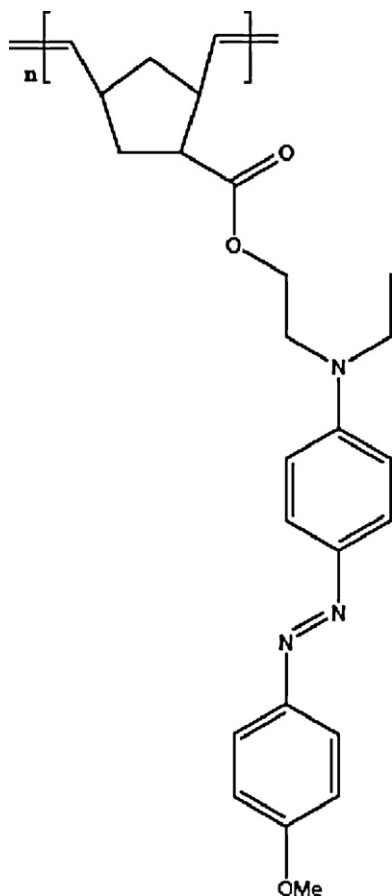


Fig. 1. A scheme represent the polymer used.

checked with indium ($T_m = 429.75 \text{ K}$, $\Delta H_m = 28.55 \text{ J g}^{-1}$) as a standard material supplied by Shimadzu. For isothermal DSC curves, samples were first heated to a fixed temperature with heating rates of 20 K min^{-1} , and then held at that temperature until a fully degraded state was achieved.

3. Results and discussion

Thermal gravimetric analysis of the polymer revealed three decompositions (Table 1) [26]. The first thermal decomposition occurs in the temperature range 523 K and 673 K which is attributed to the degradation of the azo group ($-\text{N}=\text{N}-$). It is the kinetics of this first thermal decomposition that is investigated in this article. The second thermal event occurs between 673 K and 813 K due to the decomposition of the polynorbornenes backbone, and the third decomposition occurs at temperature over 813 K.

The Johnson–Mehl–Avrami (JMA) transformation equation was first derived for transformations under isothermal annealing condition. The degradation fraction, α , can be expressed as a function of time, t , according to the JMA transformation equation [27–29]:

$$\alpha(t) = 1 - \exp[(-Kt)^n], \quad (1)$$

Table 1
Thermal gravimetric analysis data of polymer under investigation.

Segment temperature		% Weight loss
Onset (K)	End set (K)	
523	673	33
673	813	33
813	1123	33

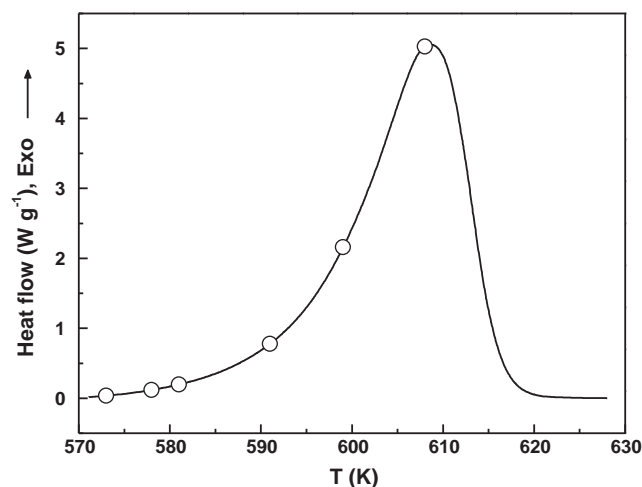


Fig. 2. Typical non-isothermal DSC trace of the polymer used measured at heating rate of 20 K min^{-1} , the figure also shows the selected temperature for isothermal studies.

where K is defined as the effective overall reaction rate constant, the variable n is the Avrami exponent. The constant K usually has Arrhenian temperature dependence:

$$K(T) = A \exp\left(-\frac{E}{RT}\right), \quad (2)$$

where $A (\text{s}^{-1})$ is the pre-exponential (frequency) factor, $E (\text{kJ mol}^{-1})$ is the effective activation degradation energy, R is the universal gas constant, and T is the absolute temperature.

The kinetic model equation combined with the Arrhenius approach to the temperature function of the reaction rate constant can generally be described by [30,31]:

$$\frac{d\alpha}{dt} = A \exp\left(-\frac{E}{RT}\right) f(\alpha), \quad (3)$$

where $f(\alpha)$ is the reaction model.

Isothermal DSC curves for the polymer were obtained at temperatures of 573, 578, 581, 591, 599 and 608 K. Fig. 2 shows these temperatures on a typical non-isothermal DSC trace obtained at 20 K min^{-1} . The DSC traces of the isothermal degradation are represented in Fig. 3. The degradation fraction was accurately determined by measuring the partial area of the peak. The classical sigmoidal curves for degraded volume versus time are constructed

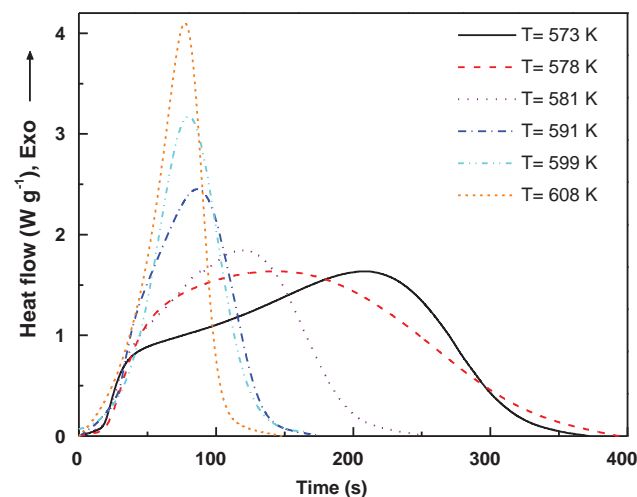


Fig. 3. Typical isothermal DSC trace of the polymer samples measured at different annealing temperatures.

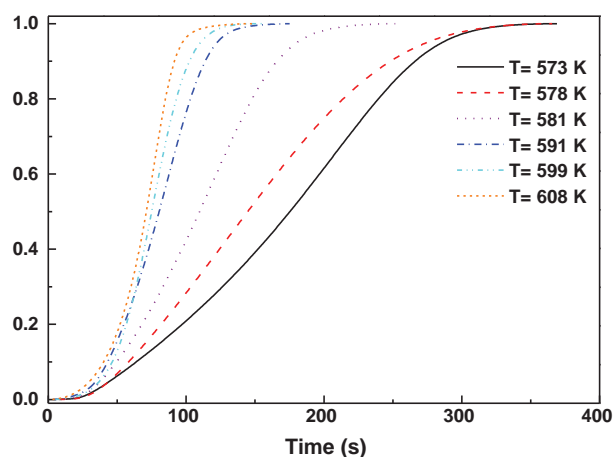


Fig. 4. The degradation fraction, α , as a function of time at different annealing temperatures.

from Fig. 3 at various annealing temperatures and are shown in Fig. 4.

Taking the logarithm of both sides of Eq. (1) twice, the following expression is obtained:

$$\ln[-\ln(1-\alpha)] - n \ln K + n \ln t. \quad (4)$$

The values of n and K are determined from Eq. (4) by the least squares fitting of $\ln[-\ln(1-\alpha)]$ versus $\ln t$ (also known as the JMA plot) as shown in Fig. 5. Values of $\ln K$ were evaluated at different temperatures by repeating the same procedure. The activation energy and frequency factor were then evaluated by the least square fitting of $\ln K$ versus $1/T$. The values of the Avrami exponent n and the overall reaction rate constant K were obtained from Fig. 5 at different annealing temperatures. Fig. 6 depicts the values of the Avrami exponent n and the overall reaction rate constant K at different annealing temperatures.

Eq. (2) was used to calculate the activation energy for the degradation, E , and the frequency factor, A , of the polymer under investigation. The plot of $\ln K$ against $10^3/T$ is shown in Fig. 7. It is evident that this data can be fitted in two regions leading to two different values of the activation energy for degradation, 140 ± 5 and $21 \pm 2 \text{ kJ mol}^{-1}$ below and above the temperature 591 K, respectively. The same behavior was recognized for the frequency factor, the two values obtained were 2.84×10^{10} and 0.793 s^{-1} for the same temperature range. The activation energy represented the energy barrier which must be overcome to transform the polymer from a stable phase into another phase. So, according to the calcu-

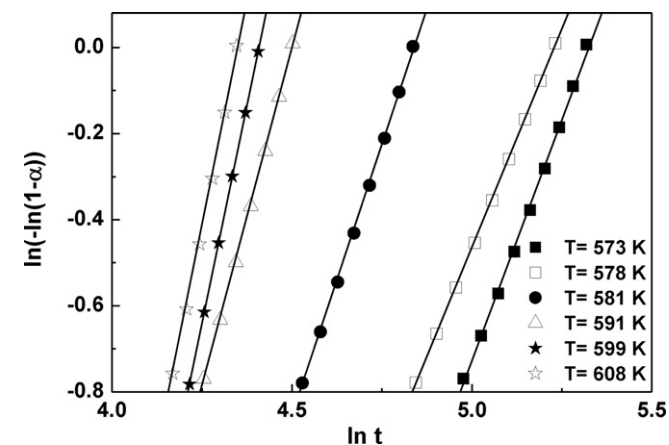


Fig. 5. Plot of $\ln[-\ln(1-\alpha)]$ versus $\ln t$ at different temperatures.

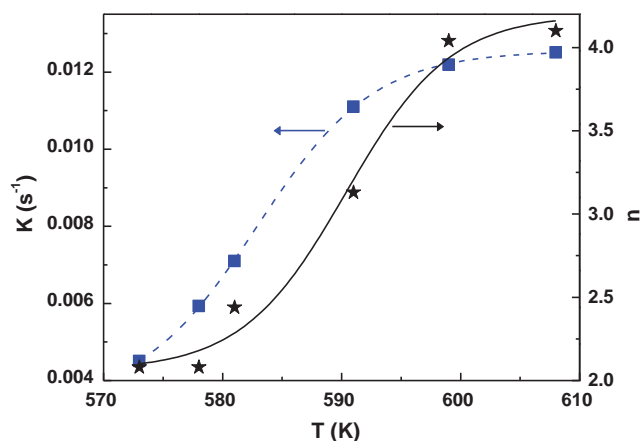


Fig. 6. Variation of the Avrami exponent, n , and the overall reaction rate constant, K , with temperature. The line represents a sigmoidal Boltzmann curve fit.

lated values of the activation energy of degradation it is extremely difficult for the azo group ($-\text{N}=\text{N}-$), to overcome the energy barrier and degrade at temperature below 591 K. This also confirmed by the frequency factor values. The result of the activation energy of azo-bond obtained at $T < 591 \text{ K}$ is comparable to the values obtained by other workers [22,25,32,33].

The temperature variation of the activation energy for degradation has always been a topic of considerable interest among kinetics. From Eqs. (1) and (2) the value of E at different temperatures can be obtained as follows:

$$E = RT \ln \left\{ \frac{At}{[\ln(1-\alpha)]^{1/n}} \right\}, \quad (5)$$

The calculated activation energies as shown in Fig. 8 are positive and initially constant at about 140 kJ mol^{-1} for annealing temperature $< 591 \text{ K}$. The activation energy drops suddenly as the temperature increases to and past 591 K to a very low constant value of approximately 21 kJ mol^{-1} . This observed drop in the activation energy may be assigned to a change in the degradation mechanism.

Therefore, to describe the degradation process more precisely, and to distinguish which one of the several kinetic models (listed in Table 2) can be used for the process, it will be useful to analyze the integral form of the reaction model, $g(\alpha)$, that is normally used to describe the kinetics of phase transformation in solids [34]. The reduced reaction model $g(\alpha)$ is given for isothermal kinetics as

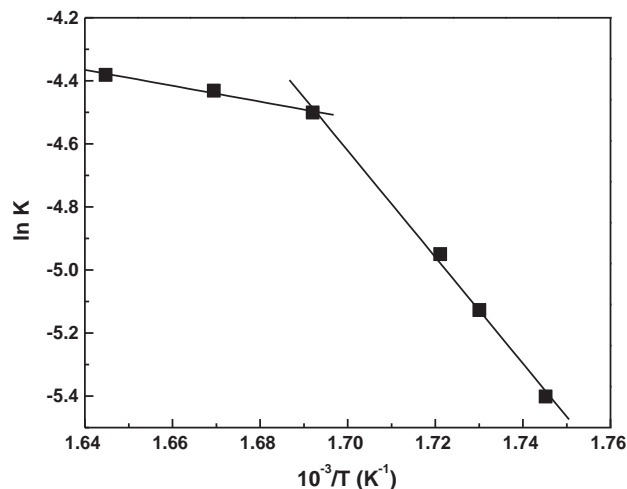


Fig. 7. Plot of $\ln K$ versus $10^3/T$ for the isothermal degradation.

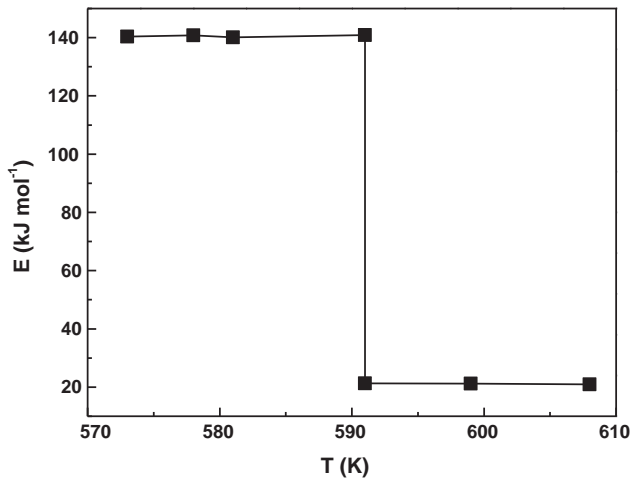


Fig. 8. Variation of the activation energy for degradation, E , with temperatures.

[35,36]:

$$g(\alpha) = \frac{t}{t_\alpha} \quad (6)$$

where t_α is the time required to reach a specific conversion, e.g. $\alpha = 0.5$. This expression is independent of the kinetic rate constants and is dimensionless.

The numerically reconstructed experimental kinetic function, $g(\alpha)$, calculated by using Eq. (6), at $\alpha = 0.632$ along with the theoretical plots for different classical models (Table 2) are presented in Fig. 9. The fractional conversion was chosen to be $\alpha = 0.632$ since in non-isothermal studies when the reduced activation energy (E/RT) approaches infinity the fractional conversion converges to $\alpha = 0.632$ at the corresponding temperature [37].

Comparison of the experimental results with those for the theoretical models can provide information on how and when the reaction mechanisms change during the course of transformation. It is very clear from Fig. 9 that the reactions follow an Avrami–Erofeev mechanism. On the other hand, and for solid state reaction models the analysis clearly indicates that the mechanism changes from A2 toward A4 as the temperature goes up. However, at a low temperature ($T = 573$ K) the mechanism closely follows A2, with a divergence toward A3 at higher stage of degradation ($\alpha > 0.7$). As the temperature approaches 591 K the mechanism closely follows A3. Though, when temperature reaches 599 K the mechanism strongly follows A4.

The variation at all degradation stages of the activation energy E can be revealed by introducing the local activation energy, $E(\alpha)$. The local activation energy, $E(\alpha)$, is obtained from the slope of the

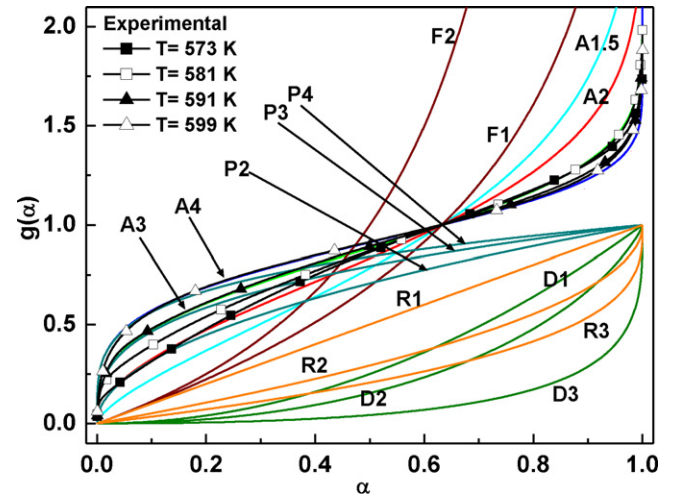


Fig. 9. The variation of the reduced reaction model, $g(\alpha)$, versus degradation fraction, α , from reduced reaction model analysis (the solid line was calculated from the various theoretical models listed in Table 2).

line $\ln(t(\alpha))$ versus $10^3/T$. During an isothermal process, the transformation time $t(\alpha)$ is related to the annealing temperature by the Arrhenius relationship [38]:

$$t(\alpha) = t_0 \exp \left[\frac{E(\alpha)}{RT} \right], \quad (7)$$

where t_0 is the time constant. The plot of $\ln(t(\alpha))$ versus $10^3/T$ at different values of degradation fraction, α , is shown in Fig. 10. Fig. 11 depicts the plot of $E(\alpha)$ versus α for the polymer under investigation concluded from Fig. 10. The figure reveals that the activation energy is not constant, but increases for two trends of activation energy, below and above 591 K. This indicates that the degradation does not take place as a one-step reaction but as a multi-step reactions, probably as competitive reactions.

In isothermal degradation the dependence of $E(\alpha)$ on α is a quite attractive. At temperature below 591 K results show that the initial stage of $E(\alpha)$ is weak and increases with increasing α . Initial stage of polymer degradation is often accompanied by melting or softening [39]. At this stage the thermal degradation can be controlled by the process of formation of a gas phase inside the polymer and by nucleation and nucleus growth in a heterogeneous medium [15]. At fast heating rate Vyazovkin and Wight [40] have reported that the concentration of nuclei is very low and the isothermal decomposition is limited by nucleation only, which takes place at lower activation energy. Thus, we may find decrease in $E(\alpha)$ at the initial degradation stages. Vyazovkin [41] reported that the shape of the

Table 2

Common solid state reaction models used to describe the degradation process.

Model notation	$g(\alpha)$	Mechanism
A1.5	$[-\ln(1-\alpha)]^{2/3}$	Avrami–Erofeev, $n = 1.5$
A2	$[-\ln(1-\alpha)]^{1/2}$	Avrami–Erofeev, $n = 2$
A3	$[-\ln(1-\alpha)]^{1/3}$	Avrami–Erofeev, $n = 3$
A4	$[-\ln(1-\alpha)]^{1/4}$	Avrami–Erofeev, $n = 4$
D1	α^2	One-dimensional diffusion
D2	$(1-\alpha)\ln(1-\alpha) + \alpha$	Two-dimensional diffusion
D3	$[-\ln(1-\alpha)]^{1/3}$	Three-dimensional diffusion (Jander)
F1	$-\ln(1-\alpha)$	First-order reaction
F2	$(1-\alpha)^{-1} - 1$	Second-order reaction
P2	$\alpha^{1/2}$	Power law, $n = 1/2$
P3	$\alpha^{1/3}$	Power law, $n = 1/3$
P4	$\alpha^{1/4}$	Power law, $n = 1/4$
R1	α	One-dimensional phase boundary reaction
R2	$1(1-\alpha)^{1/2}$	Two-dimensional phase boundary reaction
R3	$1(1-\alpha)^{1/3}$	Three-dimensional phase boundary reaction

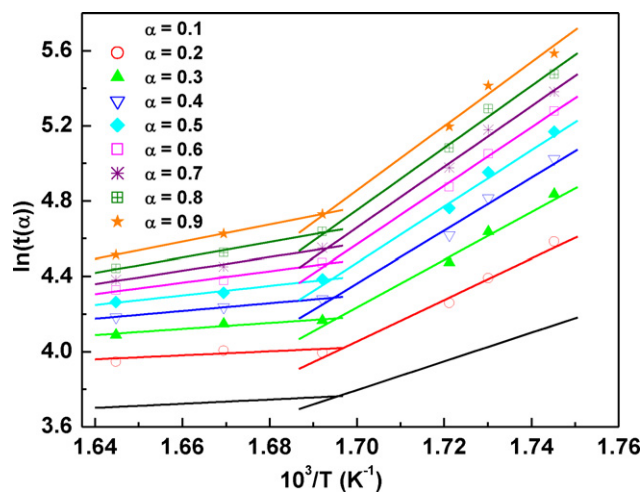


Fig. 10. The plot of $\ln(t(\alpha))$ versus $10^3/T$ at different values of degradation fraction, α .

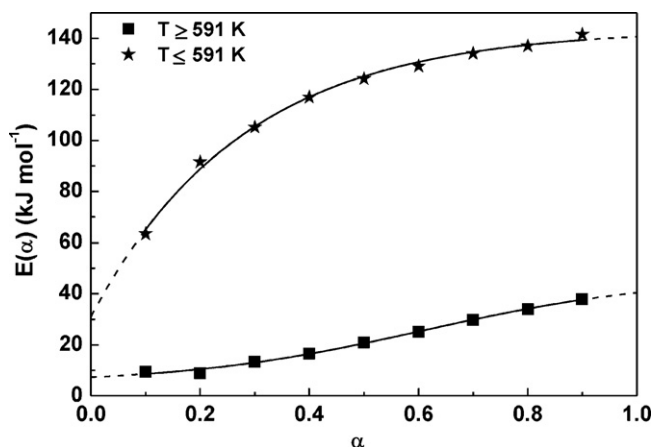


Fig. 11. Local activation energy for degradation, $E(\alpha)$, as a function of degradation fraction, α , obtained from DSC scans.

increasing dependencies of $E(\alpha)$ on α is found due to competing and some independent and consecutive reactions. Degradation temperature influences the size of the volatile products. A higher heating rate leads to degradation at higher temperature, which results in a dependence of distribution of size of volatile products on heating rate and hence the increasing of the activation energy with conversion [23]. The sudden decrease of the activation energy, $E(\alpha)$ which takes place at temperature above 591 K could be attributed to the high temperature, which is closer to the melting point.

4. Conclusions

The kinetics of an aryl azo dye-containing polynorbornene was investigated under isothermal conditions. The effect of tempera-

ture on the activation energy, preexponential factor and reaction order was investigated.

Two different values of the activation energy, 140 ± 5 and 21 ± 2 kJ mol^{-1} below and above the temperature 591 K, respectively, were obtained. The Avrami exponent, n , increases in the temperature range 573–608 K, and was observed to lie between 2 and 4. On the other hand, it can be concluded that the degradation mechanism of the polymer follows the Avrami–Erofeev mechanism with a tendency toward a multi-step reactions.

References

- [1] C. Cannizzo, S. Amigoni-Gerbier, M. Frigoli, C. Larpent, J. Polym. Sci. A: Polym. Chem. 46 (2008) 3375.
- [2] R. Fernández, I. Mondragon, P.A. Oyanguren, M. Galante, J. Reactive Funct. Polym. 68 (2008) 70.
- [3] M. Hasegawa, T. Ikawa, M. Tsuchimori, O. Watanabe, J. Appl. Polym. Sci. 86 (2002) 17.
- [4] K. Huang, H. Qiu, M. Wan, Macromolecules 35 (2002) 8653.
- [5] G. Iftime, F.L. Labarthe, A. Natansohn, P. Rochon, K. Murti, Chem. Mater. 14 (2002) 168.
- [6] A. Natansohn, P. Rochon, Chem. Rev. 102 (2002) 4139.
- [7] C. Samyn, T. Verbiest, A. Persoons, Macromol. Rapid Commun. 21 (2000) 1.
- [8] L. Wu, X. Tuo, H. Cheng, Z. Chen, X. Wang, Macromolecules 34 (2001) 8005.
- [9] S. Xie, A. Natansohn, P. Rochon, Chem. Mater. 5 (1993) 403.
- [10] G.S. Kumar, D.C. Neckers, Chem. Rev. 89 (1989) 1915.
- [11] M. Um, I.M. Daniel, B. Hwang, Compos. Sci. Technol. 62 (2002) 29.
- [12] D.M. Fernandes, A.A. Winkler Hechenleitner, E.A. Gómez Pineda, Thermochim. Acta 441 (2006) 101.
- [13] M. Wallis, S.K. Bhatia, Polym. Degrad. Stabil. 91 (2006) 1476.
- [14] B. Saha, A.K. Maiti, A.K. Ghoshal, Thermochim. Acta 444 (2006) 46.
- [15] B. Saha, A.K. Ghoshal, Thermochim. Acta 451 (2006) 27.
- [16] B. Saha, A.K. Ghoshal, Thermochim. Acta 460 (2007) 77.
- [17] P. Kannan, J.J. Biernacki, D.P. Visco Jr., J. Anal. Appl. Pyrol. 78 (2007) 162.
- [18] A. Al-Mulla, H.I. Shaban, Polym. Bull. 58 (2007) 893.
- [19] B. Saha, P. Chowdhury, A.K. Ghoshal, Appl. Catal. B: Environ. 83 (2008) 265.
- [20] Y.H. Lin, M.H. Yang, Thermochim. Acta 470 (2008) 52.
- [21] M.C. Bruns, J.H. Koo, O.A. Ezekoye, Polym. Degrad. Stabil. 94 (2009) 1013.
- [22] B. Pabin-Szafko, E. Wisniewska, B. Hefczyk, J. Zawadiak, Eur. Polym. J. 45 (2009) 1476.
- [23] R. Ramani, J. Srivastava, S. Alam, Thermochim. Acta 499 (2010) 34.
- [24] P. Krol, K. Pielichowska, L. Byczynski, Thermochim. Acta 507–508 (2010) 91.
- [25] H.H. Wu, P.P. Chu, Polym. Degrad. Stabil. 95 (2010) 1849.
- [26] A.S. Abd-El-Aziz, P.O. Shipman, P.R. Shipley, B.N. Boden, S. Aly, P.D. Harvey, Macromol. Chem. Phys. 210 (2009) 2099.
- [27] W.A. Johnson, R.F. Meh, Trans. Am. Inst. Miner. (Met.) Eng. 135 (1939) 416.
- [28] M. Avrami, J. Chem. Phys. 7 (1939) 1103.
- [29] M. Avrami, J. Chem. Phys. 8 (1940) 212.
- [30] S. Vyazovkin, N. Sbirrazzuoli, Macromol. Rapid Commun. 27 (2006) 1515.
- [31] A.A. Joraid, Thermochim. Acta 456 (2007) 1.
- [32] M. Badea, R. Olar, E. Cristurean, D. Marinescu, A. Emandi, P. Budrugaec, E. Segal, J. Therm. Anal. Calorim. 77 (2004) 815.
- [33] D. Yang, H. Ma, R. Hu, J. Song, F. Zhao, J. Mol. Struct. 779 (2005) 49.
- [34] A.A. Joraid, A.A. Abu-Selehy, M. Abu El-Oyoum, S.N. Alamri, Thermochim. Acta 470 (2008) 98.
- [35] A.C. Lua, J. Su, Polym. Degrad. Stabil. 91 (2006) 144.
- [36] S. Majumdar, I.G. Sharma, A.C. Bidaye, A.K. Suri, Thermochim. Acta 473 (2008) 45.
- [37] A. Bezjak, S. Kurajica, J. Sipusic, Croat. Chem. Acta 80 (2007) 1.
- [38] M. Avrami, J. Chem. Phys. 9 (1941) 177.
- [39] V. Mamliev, S. Bourbigot, M. Le Bras, S. Duquesne, J. Sestak, Phys. Chem. Chem. Phys. 2 (2000) 4796.
- [40] S. Vyazovkin, C.A. Wight, Chem. Mater. 11 (1999) 3386.
- [41] S. Vyazovkin, Int. J. Chem. Kinet. 28 (1996) 95.